

cDNA sequences, MALDI-TOF analyses, and molecular modelling of barley PR-5 proteins

Ernst Reiss^{a,*}, Bernhard Schlesier^b, Wolfgang Brandt^c

^a Federal Centre for Breeding Research on Cultivated Plants, Institute of Resistance Research and Pathogendiagnosics, Theodor-Roemer-Weg 4, D-06449 Aschersleben, Germany

^b Institute of Plant Genetics and Crop Plant Research, Corrensstr. 3, D-06466 Gatersleben, Germany

^c Leibniz Institute of Plant Biochemistry, Weinberg 3, D-06120 Halle (Saale), Germany

Received 15 February 2006; received in revised form 6 June 2006

Available online 31 July 2006

Abstract

Barley plants are known to produce various PR-5 proteins. Transcripts encoding eight different barley PR-5 proteins (TLPs 1–8, TLP for thaumatin-like protein) were identified and cloned – seven from infected leaves and one from developing grains. Here, we describe the cDNA sequences of four of these TLP isoforms. Moreover, the TLPs from the infected leaves (TLPs 1, 2, and TLPs 4–8) were subjected to MALDI-TOF mass spectrometric measurements that resulted in protein fragments consistent with their deduced peptide sequences. Multiple sequence alignment analysis revealed that the TLPs in barley fall into two groups: long-chain proteins (TLPs 5–8) having 16 cysteine residues and short-chain proteins (TLPs 1–4) with only 10 cysteine residues. Finally, modelling experiments highlighted the effects of sequence differences between the TLP isoforms in terms of their secondary structures and their molecular electrostatic potentials. We propose that these sequence differences have implications for the target preferences of the different isomers.

© 2006 Elsevier Ltd. All rights reserved.

Keywords: *Hordeum vulgare*; Barley pathogenesis-related proteins; PR-5 protein isoforms; Thaumatin-like proteins; cDNA; Secondary structures

1. Introduction

Plants have evolved different defence mechanisms, resulting in a large variety of structural and biochemical alterations in the plant cell. Generally, the defence responses include the activation of genes encoding proteins that have antimicrobial activity and are termed pathogenesis-related (PR) proteins (Bol et al., 1990; Van Loon, 1985). These plant defence proteins are ubiquitous in monocots and dicots and are currently grouped into 17 families based on their structural and functional properties (Van Loon and van Strien, 1999; Christensen et al., 2002).

The proteins of the PR-5 family are also called thaumatin-like proteins (TLPs) as they have a high degree of homology to thaumatin, a sweet-tasting protein from the

ripe fruits of the West African shrub *Thaumatococcus daniellii*. The TLPs are associated with diverse functions like antifungal activity (Hejgaard et al., 1991), protection against osmotic stress (Kononowicz et al., 1992), and freezing tolerance (Chun and Griffith, 1998). Moreover, some of these proteins have been reported to inhibit hyphal or spore growth of different fungi due to their ability to permeabilise the fungal plasma membrane (Roberts and Seli-trennikoff, 1990; Vigers et al., 1991). However, to date, the examination of the three-dimensional structure of PR-5 proteins has revealed few clues as to how members of this protein family form transmembrane pores and permeabilise the fungal plasma membrane (Koiwa et al., 1999).

PR-5 proteins have been suggested to bind β -1,3-glucans, and hence they might have carbohydrate-binding properties that may result indirectly in membrane permeabilisation (Trudel et al., 1998; Osmond et al., 2001). Studies on the

* Corresponding author. Tel.: +49 3473 879202; fax: +49 3473 879200.
E-mail address: e.reiss@bafz.de (E. Reiss).

molecular interaction of the tobacco PR-5 protein, called osmotin, using the yeast *Saccharomyces cerevisiae* as the model fungal genetic system, have shown that the antifungal activity of the PR-5 family of plant defence proteins may involve mechanisms resulting in pathogen apoptosis. Evidence has also been presented for a plasma membrane protein in yeast, called PHO36, that functions as a specific osmotin receptor (Narasimhan et al., 2005). Currently, the precise mode of osmotin action resulting in plasma membrane damage is not completely understood. However, some reports have indicated that the structural differences between the various isoforms of the PR-5 family are essential for the binding of different targets (Yun et al., 1997). Variations in the topology and surface electrostatic potential around the acidic cleft, commonly found in the tertiary structure of PR-5 proteins, have also been suggested to be responsible for the different specificities of the isoforms, and hence target sites in different pathogens (Min et al., 2004).

Therefore, to assess the variety of PR-5 isoforms, we present a summary of barley TLP sequences. Here, we report two new TLP sequences (TLPs 3 and 5) in barley. To date, there is conflicting literature on the numbers of the more acidic TLPs (Hahn et al., 1993; Reiss and Horstmann, 2001; EST data bank). We provide evidence to clarify this issue. Finally, to better understand the differences between the isoforms and how these affect their classification, we present structural models and discuss the implications of these differences for TLP antifungal activity.

2. Results

2.1. Two-dimensional electrophoresis

Proteins extracted from the leaves of *Drechslera teres*-infected barley plants and applied to two-dimensional polyacrylamide gel electrophoresis produced patterns of spots that were dominated by PR proteins (Fig. 1). Among them, the PR-5 proteins were identified by MALDI-TOF analyses (Fig. 2).

2.2. Acidic TLPs

Extensive screening of a cDNA library constructed from mRNA of *D. teres*-infected barley leaves for acidic TLPs resulted in the identification of three types of cDNAs encoding TLP1, TLP2, and the previously sequenced TLP4 (Gen Bank accession Nos. AY839292, AY839293, and AF355455). Additionally, a tBlastn similarity search against EST databases was carried out to better evaluate the number of acidic TLPs present in the barley genome. A short sequence region common to TLPs 1, 2, and 4 was used as query and was expected to exclude the ESTs encoding the higher molecular weight TLP isoforms. Four types of ESTs were found representing cDNAs of the previously reported TLPs 1, 2, and 4 (Reiss and Horstmann,

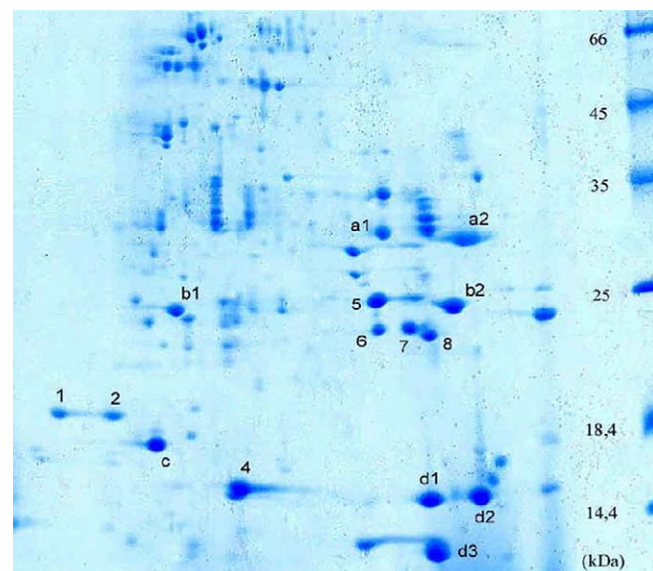


Fig. 1. Coomassie stained 2-D PAGE gel of acidic extracted barley leaf proteins. First dimension (left to right pH 3–10): IEF; second dimension (top to bottom): SDS-PAGE. The spots of the PR-5 proteins are numbered 1, 2, and 4–8 and represent TLP1, TLP2, and TLPs 4–8, respectively. Other pathogenesis-related proteins, which also have been identified by MALDI-TOF MS (data not shown), are indicated by 'a' for β -1,3-glucanases (a1 – gi|3037080, a2 – gi|809429), 'b' for chitinases (b1 – gi|563489, b2 – gi|563487), 'c' for superoxide dismutase (homologous to gi|7433318), and 'd' for the three spots of PR1 proteins (d1, d3 – gi|480679, d2 – gi|548592).

2001) plus a new cDNA expressed in the reproductive organs of barley. Using primers derived from the ESTs of the unknown TLP, PCR amplification was possible on barley genomic DNA but not on leaf cDNA (data not shown). Finally, the cDNA was cloned from dissected developing grains in glasshouse grown barley plants (cv. Mandschuria). The obtained sequence encoding a new member of barley PR5 proteins which was called TLP3 (Accession No. AY839294) according to the calculated pI of the deduced protein sequence (Table 1).

2.3. TLP5

The tryptic fragment FGGDTYCCR with a mass $m/z = 1135$ determined by MALDI-TOF analyses was common to TLPs 5, 6, and 7 (Fig. 2b). The sequence of the TLP5 fragment was also confirmed by PSD spectra (data not shown). Querying EST databases with this sequence information yielded ESTs which afterwards were screened for the known sequence of the N-terminus of TLP5 (Reiss and Horstmann, 2001). The obtained ESTs, probably encoding TLP5, facilitated the design of specific primers, which enabled PCR amplification of the cDNAs of TLP5 in samples prepared from infected leaves. The PCR product was cloned and sequenced (GenBank accession No. AY839295). The derived amino acid sequence of TLP5 was confirmed by MALDI-TOF MS data (Fig. 3) reaching a sequence coverage of nearly 97%. The TLP5 sequence

TLP1	-AT- FN IKNNCGST I WPAGIPVGGGFELGSGQT SS INVPAGTQAG RI WARTGCS FN G-G SG SCQTGDCGGQLSCS	72
TLP2	-AT- FN IKNNCGST I WPAGIPVGGGFELGSGQT SS INVPAGTQAG RI WARTGCS FN G-G SG SCQTGDCGGQLSCS	72
TLP3	TSTPL TI TNRCSFT V WPAVAPAGLGT EL HPGAN WS VDES AF DS PA SIW GR TGCS FD AAG SGL CRTADCGSGLRCA	75
TLP4	-RS- FS ITNRCSFT V WPAATPVGGGRQLNGGET WN LDIPDGTSS AR IW GR TDC SF NG- NS GRCGTGDCGGALSCT	72
Zeam	-AV- FT VVNQCPFT V WAASVPVGGGRQLNRGES WR ITAPAGTT AR IWARTG CK FDAS RG SCRTGDCGGVLQCT	73
TLP1	LSGQP-PATL AE FTIGGGSTQ DFY DISVI-D-GFN LAMD F----- SC STGD ALQ C-----RDPS-----	118
TLP2	LSGRP-PATL AE FTIGGGSTQ DFY DISVI-D-GFN LAMD F----- SC STGD ALQ C-----RDPS-----	118
TLP3	TTDPAPV TR AQ V ASSEG---F YH YG IT TDKG FN L PLD L----- TC SSGD ALR C-----REEG-----	120
TLP4	LSGQP-PLTL AE FT L GGG-- TDFY DISVI-D-GYN LPMD F----- SC STGV NIQ C-----RDRN-----	116
Zeam	GYGRA-PNTL AE YALKQ FNN LD FFD ISLI-D-GFN VMS FLPDGGS-G CS RGP-- RC AVDVNARCP AE LRQDGVC	143
TLP1	-----3758----- CP PPQAYQH PND V ATH ACSGNNN- YQ IT FC P-----	153
TLP2	-----3758----- CP PPQAYQH PND V ATH ACSGNNN- YQ IT FC P-----	153
TLP3	----- CH DAFPYVE FN E--- HAC TAAGSR LQ IV FC P-----	153
TLP4	-----1526----- CP DAYHT PP EP KT K-- AC SG-NRR FN IV FC P-----	149
Zeam	NN AC PV FK KDEYCC V SA AND CH PT N YS RY FK GQ CP DAYSYPKDD AT ST FT CPAGTN- YK V V FCP-----	206

Fig. 2a. CLUSTAL W (V.1.82) multiple sequence alignment of the barley PR-5 proteins (TLP1–4) and zeamatin (Zeam) using MOE with alignment constraints (underlined cysteins). Bold highlighted letters indicate α -helical, and bold and cursive letters β -sheet secondary structures. The fragment masses of the TLPs measured by MALDI-TOF mass spectrometry were assigned to the sequences. The masses were rounded up to obtain whole digits. ‘|’ marks the cleavage sites of the tryptic digestion C-terminal at arginine and lysine.

shows a high degree of similarity to the sequences of TLP6 and TLP7 (Fig. 2b).

2.4. Molecular modelling of barley TLPs

Homology modelling for TLPs 5–8 is based on the alignment with the X-ray structure of 1DU5 (maize zeamatin) (Batalia et al., 1996). Since template and target proteins have nearly the same sequence lengths and no large gaps in their alignment, the resulting secondary structures of TLPs 5–8 are almost identical to 1DU5. This is also indicated by the eight conserved disulphide bridges listed in Table 2. Much more difficult was the modelling of TLPs 1–4. These four proteins contain only ten cysteine residues which allows in maximum only the formation of five disulphide bridges instead of the eight bridges in TLPs 5–8 and 1DU5. Furthermore, the alignment with 1DU5 shows a large gap (residues 112–150 in 1DU5), which causes problems in simple protein homology modelling. Using standard settings (BLOSUM50) with several different gap penalties no appropriate model could be formed which allowed the formation of five disulfide bridges. With the help of alignment constraints between the cysteins of the TLPs and 1DU5 using MOE (molecular operating environment) models could be created which very likely represent a native-like fold of these four proteins. In the alignment

shown in Fig. 2a the cysteine residues with applied alignment constraints are accentuated (underlined). In Table 2 the z-score values are also listed resulting from the PROSA II analysis (Sippl, 1990). All the z-scores of TLPs 1–4 are a bit smaller than the mean values expected for proteins with the corresponding sequence length of 1DU5, but in the tolerance given by PROSA II. The modelled structures have been accepted by the protein database and in Table 2 their entry-codes are listed for downloading (<http://www.rcsb.org/pdb/Welcom.do>) and detailed inspection. The structures of TLP1 and TLP5 are exemplified in Fig. 4. Whereas the structure of TLP5 is almost identical to the experimental template 1DU5, the helical domain of TLP1 is completely removed. The secondary structure of all proteins is characterised by an extended beta sheet in the centre of the proteins. The first four TLPs (TLPs 1 to 4) do not form any other secondary structure element. In contrast, within the other four TLPs (TLPs 5–8), there is at least one helix at the left hand side of the structures. These differences can also be seen in the sequence alignment (Fig. 2) and correspond to about 50 amino acid residues inserted in TLPs 5–8 in comparison to TLPs 1–4. Corresponding to the shown orientation of the secondary structure for each protein, the molecular electrostatic potentials at the Connolly surface (spatially accessible surface of a water molecule with a van der Waals radius of

	904		1663		1970		557		856		1453		
TLP5	-TT-	ITVVNR	CSYTIWPGALP-	GGGARLD	PGQ SWQL	NMPAGTAGARVWP	RTG CTF	DRSGR GRC	ITGDCAGALVCR				72
	873		1677		1913		1057		1496				
TLP6	-AT-	ITVVNR	CSYTVWPGALP-	GGGVRLD	PGQ SWAL	NMPAGTAGARVWP	RTG CTF	DGSG RGRC	ITGDCNGVLACR				72
	873		1677		1913		1057		1411				
TLP7	-AT-	ITVVNR	CSYTVWPGALP-	GGGVRLD	PGQ SWAL	NMPAGTAGARVWP	RTG CTF	DGSG RGRC	ITGDCGGALACR				72
	894		1764		1931		1198		982				
TLP8	-AT-	FTVINK	CQYTVWAAAVPAGGGQ	KLDAGQ	TWSIN	PAGTTSGRVW	ARTG CSF	DGAG NGRC	QTGDCGGKLRCT				73
Zeam	-AV-	FTVVNQ	CPFTVWAAAVPVG	GGRQL	NRGESW	RI	TAPAGTTAARI	WARTG CKF	DASGRG SC	RTGDCGGVLQCT			73
	2048		2872		2972								
TLP5	VS	GEQ-PAT	LA EYTLGQGGNR DFDL	SLIDGFNV	PM SFQ PVGGA-PCRAA--	TC	AVDITHECLPELQV	PGGCASA					143
	2063		2705		1434								
TLP6	VSG	QQ-PTT	LA EYTLGQGGANK DFDL	SLIDGFNV	PM SFEP VGG---CRAA--	RC	ATDITKDCLELQV	PGGCASA					141
	2063		2806		1434								
TLP7	VSG	QQ-PTT	LA EYTLGQGGANK DFDL	SLIDGFNV	PM SFEP VGAS---CRAA--	RC	ATDITKECLELQV	PGGCASA					143
	2012		1270		1370								
TLP8	QY	GQA-PNT	LA EFGLNKYM QDF	DISLIDGYN	VM SFVP APGSTGCPKGGPRCPKVIT	PAC	PNELRAAG	GCMNA					147
Zeam	GY	GRA-PNT	LA EYALK QFNN	L DF DISLIDGYN	VM SFLP DGGS-GCSRG-PRCAVDVNARCPAEL	RQ	DGVCNNA						145
	1135		1756		1074		2615						
TLP5	CGK FGGDTYCCRG QFEH	NCPP	TY SR FFK GKCPDAYS	YAKDDQ	TS FT CPA-GTNY	QIV LC	PARNDLHMDQ						213
	1135		1074										
TLP6	CGK FGGDTYCCRG QFEH	NCPP	TY SM FFK GKCPDAYS	YAKDDQ	TS FT CPA-GTNY	QIV LC	-----						202
	1135		1679		1074								
TLP7	CGK FGGDTYCCRG QFEH	NCPP	TY SK FFK GKCPDAYS	YAKDDQ	TS FT CPA-GTNY	QIV LC	-----						203
	2027		1286										
TLP8	CTVFKEDRYCCTGSAANS	CGPTD	YSR FFK GQCPDAYS	YPKDDAT	S IFT CPG-GTNY	QVIF CP	-----						208
Zeam	CPV FKKDEYCCVGS	AANDCH	PTNYSR	YFKGQCPDAYS	YPKDDAT	S FT CPA-GTNY	KVV FCP	-----					206

Fig. 2b. CLUSTAL W (V.1.82) multiple sequence alignment of the barley PR-5 proteins (TLP5–8) and zeamatin (Zeam). Bold highlighted letters indicate α helical, and bold and cursive letters β -sheet secondary structures. The fragment masses of the TLPs measured by MALDI-TOF mass spectrometry were assigned to the sequences. The masses were rounded up to obtain whole digits. ‘|’ marks the cleavage sites of the tryptic digestion C-terminal at arginine and lysine.

1.4 Å) are represented (Fig. 5). The molecular electrostatic potentials of TLPs 5–8 show a negatively charged cleft caused by acidic residues (two aspartic acid and one glutamate), which may represent a binding site for not yet known ligands. Such a negatively charged cleft is not so distinctive for TLPs 1–4. In particular, TLP3 is clearly different from the other TLPs because it is lacking the acidic residues in identical positions. This results in a different form of the pocket and weaker negative potentials in this area which might be an indication of altered substrate spec-

ificity of this protein. An observation that certainly deserves further analysis in future work.

When comparing the sequences of all TLPs, TLP5 turns out to be the longest protein with nine additional residues at the C-terminus. This chain extension could not be modelled due to the lack of a structural template. However, the C-terminus is located at the opposite site of the acidic cleft. Therefore, an extension of the chain in this position will very likely not influence the putative pocket for any ligand binding.

Table 1
Data calculated from the sequences of the cloned cDNAs of barley TLPs

	GenBank locus	Molecular mass (Da)	Theoretical pI acc. Expasy	Mature peptide (aa)	Cysteine residues
TLP1	AY839292	15626	4.33	153	10
TLP2	AY839293	15654	4.51	153	10
TLP3	AY839294	16071	4.85	153	10
TLP4	AF355455	15873	5.71	149	10
TLP5	AY839295	22724	6.24	213	16
TLP6	AF355456	21352	7.53	202	16
TLP7	AF355457	21379	7.91	203	16
TLP8	AF355458	21855	8.15	208	16

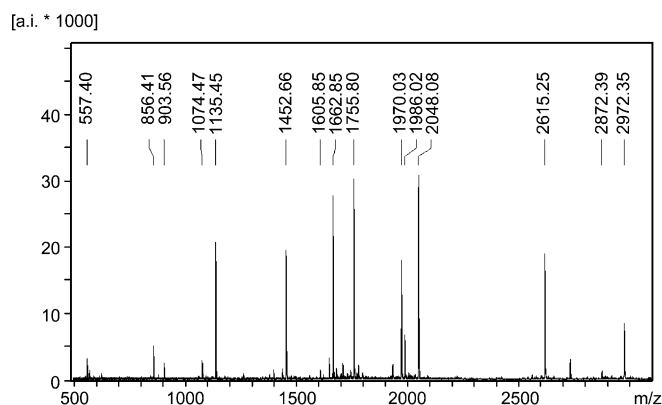


Fig. 3. Tryptic peptide mass fingerprint of TLP5. The 15 labelled masses match with the peptide fragments as according to Fig. 2. All cysteines have been modified with iodoacetamide to form carbamidomethyl-cysteine. Additionally, the mass $m/z = 1605.85$ indicates the non-derivatised peptide fragment from position 9 to 24, and the mass $m/z = 1986.02$ indicates the oxidation of the methionine residue to the sulfoxide (MSO) in the peptide fragment from position 25 to 43.

3. Discussion

3.1. The array of TLP sequences

Transcripts encoding eight different barley PR-5 proteins were identified and cloned – seven from infected leaves and one from developing grains. TLPs 1 to 4 belong to the group of smaller PR-5 proteins, which are found mainly in the cereals. However, in chickpea, PR-5a is only 16 kDa, and was the first smaller PR-5 member to be described in dicots (Hanselle et al., 2001). TLPs 1 and 2 differ only in one amino acid residue and represent the stronger acidic TLPs, whereas TLPs 3 and 4 are moderately acidic and belong to the PR-like proteins since TLP3 was not detected in infected leaves and TLP4 was found in both healthy and infected leaves. In this study, the configuration (grouping) of TLPs 1 to 4 contrasts with those of previous findings of four acidic (three strongly and one weakly) members from infected leaves (Reiss and Horstmann, 2001) as well as with the cDNA cloning of three strongly acidic isoforms from *Rhynchosporium secalis*-infected bar-

ley leaves (Hahn et al., 1993). In the first case, the previously described third spot at the stronger acidic region of the gel may have been resulted from insufficient reduction/alkylation before isoelectric focusing. In the second case, the cDNAs of PR-Hv1a and PRHv1b both seem to encode only the one stronger acidic TLP1, whereas TLP2 was encoded by PR-Hv1c.

3.2. Posttranslational modifications of the proteins were not detected

The MALDI-TOF analyses of TLPs from the infected barley leaves resulted in fragments which are in perfect accordance with the sequences translated from cDNA sequences. Therefore, posttranslational modifications of the proteins were not detected. A fragment of TLP7 with a potential motif for *N*-glycosylation at position N-165 was present only in its native, unmodified form, indicating that glycosylation has not taken place. The corresponding fragment from TLP6 with a similar potential *N*-glycosylation site at N-164 could not be detected, but this maybe because this fragment is more difficult to transfer into a detectable ionised state. However, the location of the spots of TLPs 6 and 7 in the 2D PAGE gel in relation to their molecular weights would not favour extensive glycosylation of TLP6.

All of the identified barley PR-5 proteins contain an N-terminal signal sequence for export to the apoplast. The traditional subdivision of some PR protein families into acidic proteins, which are secreted, and basic proteins, which remain in the cells, appears not to apply to the TLPs of barley. Therefore, in intercellular washing fluids of stressed barley leaves, basic as well as acidic PR-5 proteins are detected (Trudel et al., 1998). TLP5 shows a C-terminal structure differing from that of the other TLPs. This kind of C-terminal extension has been suggested to be a vacuolar sorting determinant (Neuhaus and Rogers, 1998). Interestingly, there are some indications of the presence of modified TLP5 proteins at certain sites in the 2D-PAGE which are different from those detected by MALDI-TOF analyses of the protein spots shown in Fig. 1 (unpublished data). However, to date, no modified fragments have been detected lacking the nine amino acid C-terminal extension.

Table 2
Disulfide bridges and *z*-scores of the modeled structures

Protein	Disulphide bridge 1	Disulphide bridge 2	Disulphide bridge 3	Disulphide bridge 4	Disulphide bridge 5	Disulphide bridge 6	Disulphide bridge 7	Disulphide bridge 8	<i>z</i> -Score	<i>z</i> -Score-mean	Sequence length	pdb-code
1DU5	9–205	51–61	66–72	118–194	124–177	132–142	146–155	156–164	–8.32	–9.57	206	1DU5
TLP1	9–153	51–60	65–71	111–141	119–124	–	–	–	–6.88	–8.83	153	2DOV
TLP2	9–152	51–60	65–71	111–141	119–124	–	–	–	–7.32	–8.83	153	2DOW
TLP3	12–153	54–64	69–75	114–141	122–127	–	–	–	–6.67	–8.80	151	2DOZ
TLP4	9–148	51–60	65–71	109–137	117–122	–	–	–	–7.06	–8.77	149	2DOX
TLP5	9–203	50–60	65–71	117–192	122–175	130–140	144–153	154–162	–7.82	–9.55	204	2DOY
TLP6	9–201	51–61	65–71	115–190	120–173	128–138	142–151	152–160	–8.18	–9.51	202	2DP1
TLP7	9–202	50–60	65–71	116–191	121–174	129–139	143–152	153–161	–8.62	–9.53	203	2DP2
TLP8	9–207	51–61	66–72	119–196	126–179	134–144	148–157	158–166	–8.39	–9.60	208	2DP0

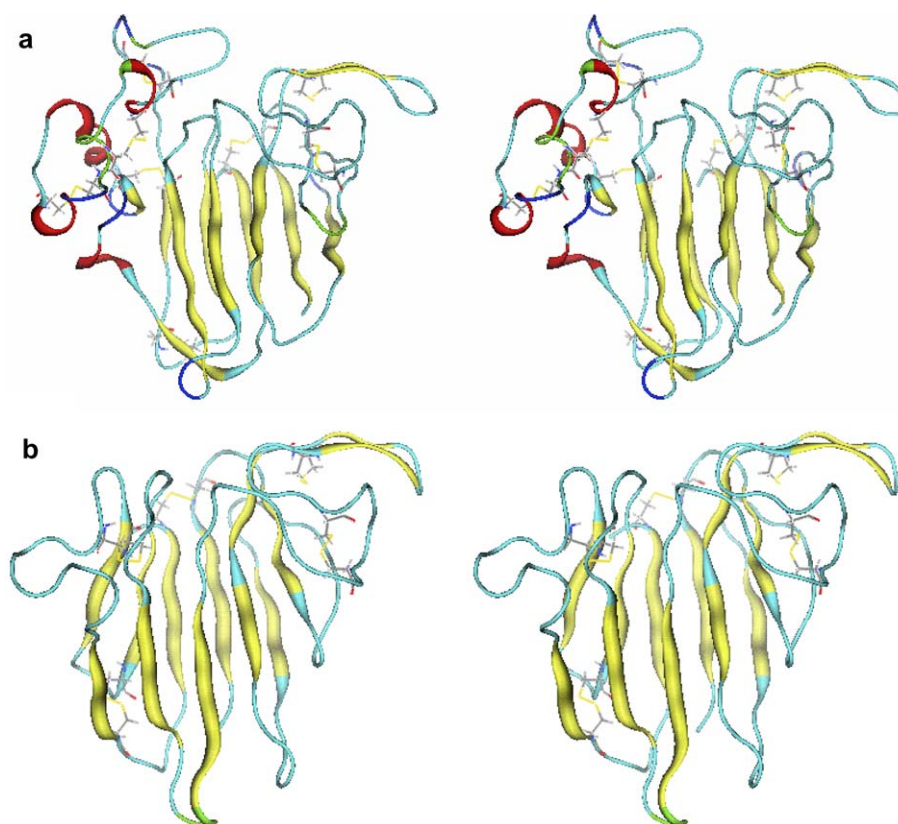


Fig. 4. Stereo-representation of the secondary structure of TLP5 (a) and of TLP1 (b) with shown disulfide bonds. Yellow arrows indicate beta sheets, red alpha helices, and light blue coil loop structures.

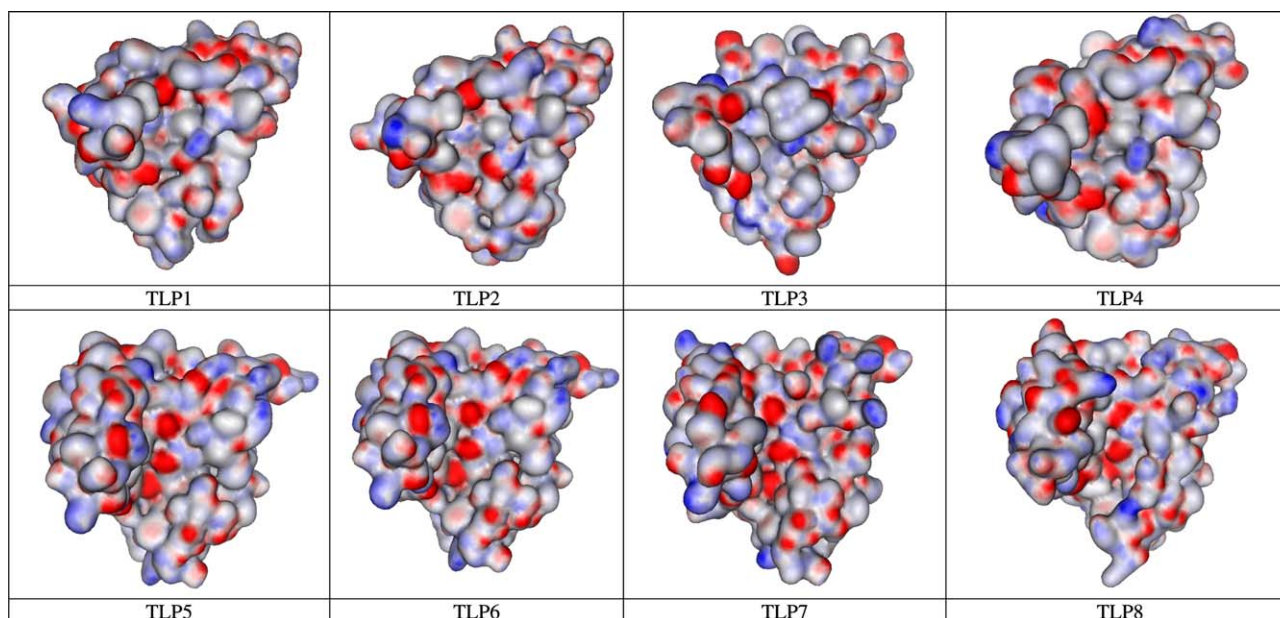


Fig. 5. Representation of the molecular electrostatic potentials of TLP1 to TLP8 for comparison. Red areas of the potential indicate acidic (negative) and blue ones basic (positive) electrostatic potential. The view is identical to the shown structures in Fig. 3.

Moreover, the existence of a C-terminal structure different from that of related proteins is not sufficient to conclude that this extension results in different targeting. For exam-

ple, class II and IV chitinases differ at their C-termini by six to nine amino acids but are still both secreted (Neuhaus et al., 1996).

3.3. Secondary structures and surface electrostatic potentials

Modelling of the barley TLPs revealed clear differences in the overall peptide structures. As already proposed for the cDNA sequences, the described isoforms of barley PR-5 proteins can be classified roughly into those having the normal size of most PR-5 proteins, characterised by eight disulphide bonds, and those which are shortened to peptide structures containing only five disulphide bonds. These deletions in TLPs 1–4 result in simpler peptide structures without the alpha helices found in TLPs 5–8. In principle, the size of the proteins or the presence of alpha helices seems not to be decisive for the antifungal activity since the small TLP2 from winter rye, which has 96% identity to barley TLP2, has been described to possess antifungal activity towards some fungal species (Chan et al., 1999).

Barley TLP proteins R and S (corresponding to TLP6/TLP7 and TLP8, respectively) have been reported to inhibit fungal growth in vitro (Hejgaard et al., 1991). A common motif of PR-5 proteins seems to be the conserved cleft region, which is highly acidic in all the barley TLPs except TLP3. All of the known antifungal PR-5 proteins are similar in their acidic cleft regions, whereas thaumatin has no antifungal activity and its cleft is basic (Min et al., 2004). Taken together, this suggests that the negative charges in the cleft regions may be crucial in conferring antifungal activity.

In addition, PR-5 proteins show different activities and specificities against their target cells (Selitrennikoff, 2001; Yun et al., 1998; Wang and Ng, 2002). The predicted secondary structures for both TLP subgroups in barley have many differences, the significance of which, however, can only be clarified once we know the still to be determined interacting molecules. The difference between the TLPs 1 and 2 is due to a single amino acid which results in a protruding basic group above the acidic cleft in TLP2. Such small differences in the proposed topology and surface electrostatic potential around the acidic cleft and in other structural regions of the barley TLPs have to be considered as determinants for the various specificities of the TLPs towards target fungal cells. For instance, when comparing TL8 with the other basic TLPs 5–7, the differently positioned basic groups near the acidic cleft are clearly visible, indicating that these areas will have different bonding preferences. The initial interaction of TLPs with the fungal cell wall surface may be facilitated by the hydrophilic back of the proteins, which is highly basic, especially in the group of large TLPs. Experimental binding data for selected single-stranded (1,3)- β -D-glucans to the acidic clefts of HvPR5b and HvPR5c (corresponding to TLPs 8 and 6, respectively) have shown that the different ability to form hydrogen bond interactions with the carbohydrate group might explain why HvPR5c binds (1,3)- β -D-glucans and why HvPR5b does not (Osmond et al., 2001). For a better understanding of the role of different barley PR-5 isoforms, more information about putative receptor targets located

in the fungal cell membrane and cell wall is needed in order to exploit the information on TLPs provided here for secondary structures and molecular electrostatic potentials in further docking experiments.

4. Experimental

4.1. Plant material

Culture and infection of barley (*Hordeum vulgare* L. cv. Karat) plants with *Drechslera teres* f. *teres* and the acidic extraction of the leaf proteins were described previously (Reiss and Bryngelsson, 1996). Generally, the primary leaves of the young seedlings were used for the analyses. To analyse the expression of TLP3 in the reproductive organs of barley, the developing grains of barley cv. 'Mandschura' were separated as a whole 3–6 days after anthesis and RNA was extracted. All plants were grown under greenhouse conditions.

4.2. Two-dimensional gel electrophoresis (2D-E)

Isoelectric focusing (IEF) with immobilised pH gradients (Goerg et al., 2000) and sodium dodecyl sulphate-polyacrylamide gel electrophoresis (SDS-PAGE) were carried out essentially as recommended by the manufacturers. Crude protein extracts were purified for preparing low conductivity samples by using the Perfect FOCUS kit (GenoTech, St. Louis, MO, USA). Isoelectric focusing was performed using the PROTEAN IEF system with immobilised pH gradients (IPG) for 2D-E (Bio-Rad, Munich, Germany). The pellets of the purified proteins obtained from 1 g leaf material were dissolved in the supplied rehydration buffer containing 50 mM DTT. Dehydrated 11 cm IPG strips (pH 3–10, linear) were rehydrated overnight in 185 μ l rehydration buffer. Focusing was performed in three steps: 1. 500 V for 1 h, 2. 1000 V for 1 h, and 3. 8000 V until 7500 Vh were reached. The current limit was set to 50 μ A per strip. Focused IPG strips were stored at -20°C overnight and afterwards equilibrated for the second dimension in two steps: 1. with equilibration-base buffer mixed with 2% DTT and 2. with equilibration-base buffer mixed with 5% iodoacetamide. The strips were placed on the top of a 15% SDS-PAGE gel with 3% stacking gel and overlaid with 0.5% (w/v) low melting agarose prepared in running buffer. The gel was run in the second dimension at 25 mA using the PROTEAN II xi Cell system (Bio-Rad, Munich, Germany). The protein spots were visualised by staining with Deep Blue - Colloidal Coomassie (MoBiTec, Göttingen, Germany).

4.3. MALDI-TOF MS

In-gel digestion and MALDI-TOF MS analysis of the TLP-samples were carried out as described previously (Schlesier et al., 2004).

4.4. Nucleic acid isolation and PCR

Standard molecular biology techniques were carried out as described previously (Ausubel et al., 1999). For RNA isolation, cDNA preparation, and preparation of genomic DNA respective kits were used (Qiagen, Hilden, Germany). PCR amplification for TLP5 was performed using the forward primer 5'-CAGCACCAAACCACCATATTCAAACAAG-3' and the reverse primer 5'-GAGCGGCCACCC (T)₃₀-3'. To amplify the sequence of TLP3 from the genomic DNA, the following primer pair was used: 5'-ACCGACCCCCCGGCGCCGGTGAC-3' as forward primer and 5'-GCTCATCATGGGCAGAAGACGATCTGGAGCAGG-3' as reverse primer. For amplifying TLP3 in cDNA isolated from developing grains 5'-GTTCCACAAAATGGCTCGCGCCTCTC-3' as forward primer and 5'-GAGCGGCCACCC(T)₃₀-3' as reverse primer were used. The PCR program used to amplify both TLPs consisted of a 94 °C hot start for 5 min, followed by 30 cycles of denaturation (94 °C, 45 s), annealing (60 °C, 45 s), and extension (72 °C, 1 min). This was followed by a final 10 min extension at 72 °C. PCR products were fractionated on a 1.5% agarose gel and the expected size bands were cut out and purified using the High Pure PCR Product Purification kit (Roche Applied Science, Penzberg, Germany).

4.5. Cloning and sequencing of nucleic acids

Purified DNA of PCR products was cloned in pDrive Cloning Vector (Qiagen, Hilden, Germany). Transformation and plating were performed according to the recommendations of the manufacturer.

The cDNA library was produced from mRNA of barley leaves 5 days after inoculation with *D. teres* f. *teres* as described (Reiss and Horstmann, 2001). The plasmid DNA was prepared using the Qiaprep system (Qiagen) and then applied to fluorescent sequencing (Amersham Biosciences, Freiburg, Germany).

4.6. Bioinformatics (Identification by database search)

The computer analyses of the nucleotide and amino acid sequences were performed with the PCGENE software (Release 6.85, IntelliGenetics, Geneva, Switzerland) and with the ExPASy Proteomics Server (<http://us.expasy.org/>). For screening EST databases, the Blast server of NCBI was used, and for the tBLASTn search, the Blast server in the bioinformatics tools of the Plant Genome Resource Centre of the Institute of Plant Genomics and Crop Plant Resource in Gatersleben, Germany was used. In the search for TLP5, the peptide sequence FGGHDTYCCR was used in tBLASTn (Altschul et al., 1990) and the obtained ESTs were selected successfully with the TLP5 N-terminus TTITVVNRCSYTIW. The search for the smaller TLP isoforms of barley by tBLASTn was performed using the sequence FNLAMDFSCSTDAL as a query and the tBLASTn search in EST data

bank for additional, up to now not described TLPs was performed with the query NXCXXTXWXXXXPXGXG-XXLXXGXXXXXXXXXXXXXXXXXXWXRXCXFFX-XXXGXCXTXDCXXLXC (X represents any amino acid residue).

4.7. Molecular modelling

To find homologous proteins with known three-dimensional structures to the eight thaumatin-like proteins (TLPs) of barley (*Hordeum vulgare*), a Blastp (Altschul et al., 1990) search was used. The program provided as the most promising template structures for homology modelling IPCV (tobacco osmotin) (Min et al., 2004), 1DU5 (maize zeamatin) (Batalia et al., 1996), 1AUN (tobacco PR-5 d) (Koiwa et al., 1999), 1THU (thaumatin b) (Ko et al., 1994), and 1RQW (thaumatin) (Ma and Sheldrick, unpubl.) with E-values below 10^{-27} . The sequence identities between the templates and target structures was approximately 50% which is sufficient for homology modelling.

The program MOE© (Molecular Operating Environment) was used for homology modelling of the eight TLPs. The sequences were aligned with the aforementioned templates using the blosum 50-matrix (Henikoff and Henikoff, 1992, 1993). For each protein, ten models have been calculated by MOE and pre-optimised using the Charmm force field (MacKerell et al., 1998). All ten models were checked with regard to stereochemical quality using PROCHECK (Laskowski et al., 1993). The backbone dihedral angle distribution of all amino acid residues (Ramachandran Plot) showed on average 86% in most favoured, 11% in additional allowed, and 3% in generously allowed regions. All other stereochemical parameters were inside the quality expected for a structure with a resolution of 2.0 Å. The quality of the fold was inspected with PROSA (Sippl, 1990) that allowed all residues in negative energy regions very similar to the template protein, and indicates the possible correctness of the modelled structures.

Molecular electrostatic potentials were calculated at the Connolly surface (Connolly, 1983a,b) of the proteins using MOLCAD (Heiden et al., 1993) and Gasteiger charges (Gasteiger and Marsili, 1980), which are implemented in the SYBYL molecular modelling package (SYBYL© Tripos Associates Inc.) at Silicon Graphics workstations.

Acknowledgements

Excellent technical assistance of Ursula Apel and Annegret Wolf is acknowledged. We thank Dr. Patrick Schweizer, IPK Gatersleben, for critical reading of the manuscript.

References

- Altschul, S.F., Gish, W., Miller, W., Myers, E.W., Lipman, D.J., 1990. Basic local alignment search tool. *J. Mol. Biol.* 215, 403–410.

- Ausubel, F.M., Brent, R., Kingston, R.E., Moore, D.D., Seidmann, J.G., Smith, J.A., Struhl, K. (Eds.), 1999. Current Protocols in Molecular Biology. John Wiley & Sons, New York.
- Batalia, M.A., Monzingo, A.F., Ernst, S., Roberts, W., Robertus, J.D., 1996. The crystal structure of the antifungal protein zeamatin, a member of the thaumatin-like, PR-5 protein family. *Nat. Struct. Biol.* 3, 19–23.
- Bol, J.F., Linthorst, H.J., Cornelissen, B.J., 1990. Plant-pathogenesis-related proteins induced by virus infection. *Annu. Rev. Phytopathol.* 28, 113–138.
- Chan, Y.W., Tung, W.L., Griffith, M., Chow, K.C., 1999. Cloning of a cDNA encoding the thaumatin-like protein of winter rye (*Secale cereale* L. Musketeer) and its functional characterization. *J. Exp. Bot.* 50, 1627–1628.
- Christensen, A.B., Cho, B.H., Næsby, M., Gregersen, P.L., Brandt, J., Madriz-Ordeñana, K., Collinge, D.B., Thordal-Christensen, H., 2002. The molecular characterisation of two barley proteins establishes the novel PR-17 family of pathogenesis-related proteins. *Mol. Plant Pathol.* 3, 135–144.
- Chun, J.U., Griffith, M., 1998. Variation of the antifreeze proteins during cold acclimation among winter cereals and their relationship with freezing resistance. *Korean J. Crop Sci.* 43, 172–178.
- Connolly, M.L., 1983a. Analytical molecular surface calculation. *J. Appl. Crystallogr.* 16, 548–558.
- Connolly, M.L., 1983b. Solvent-accessible surfaces of proteins and nucleic acids. *Science* 221, 709–713.
- Gasteiger, J., Marsili, M., 1980. Iterative partial equalization of orbital electronegativity - a rapid access to atomic charges. *Tetrahedron* 36, 3219–3228.
- Goerg, A., Obermaier, C., Boguth, G., Harder, A., Scheibe, B., Wildgruber, R., Weiss, W., 2000. The current state of two-dimensional electrophoresis with immobilized pH gradients. *Electrophoresis* 21, 1037–1053.
- Hahn, M., Jüngling, S., Knogge, W., 1993. Cultivar-specific elicitation of barley defense reactions by the phytotoxic peptide NIP1 from *Rhynchosporium secalis*. *Mol. Plant Microbe Interact.* 6, 745–754.
- Hanselle, T., Ichinose, Y., Barz, W., 2001. Biochemical and molecular biological studies on infection (*Ascochyta blight*)-induced thaumatin-like proteins from chickpea plants (*Cicer arietinum* L.). *Zeitschr. Naturforsch. C* 56, 1095–1107.
- Heiden, W., Moeckel, G., Brickmann, J., 1993. A new approach to analysis and display of local lipophilicity/hydrophilicity mapped on molecular surfaces. *J. Comput. Aided Mol. Des.* 7, 503–514.
- Hejgaard, J., Jacobsen, S., Svendsen, I., 1991. Two antifungal thaumatin-like proteins from barley grain. *FEBS Lett.* 291, 127–131.
- Henikoff, S., Henikoff, J.G., 1992. Amino acid substitution matrices from protein blocks. *Proc. Nat. Acad. Sci. USA* 89, 10915–10919.
- Henikoff, S., Henikoff, J.G., 1993. Performance evaluation of amino acid substitution matrices. *Proteins Struct. Funct. Genet.* 17, 49–61.
- Ko, T.P., Day, J., Greenwood, A., McPherson, A., 1994. Structures of 3 crystal forms of the sweet protein thaumatin. *Acta Crystallogr. D. Biol. Crystallogr.* 50, 813–825.
- Koiwa, H., Kato, H., Nakatsu, T., Oda, J., Yamada, Y., Sato, F., 1999. Crystal structure of tobacco PR-5d protein at 1.8 Å resolution reveals a conserved acidic cleft structure in antifungal thaumatin-like proteins. *J. Mol. Biol.* 286, 1137–1145.
- Kononowicz, A.K., Nelson, D.E., Singh, N.K., Hasegawa, P.M., Bressan, R.A., 1992. Regulation of the osmotin gene promoter. *Plant Cell* 4, 513–524.
- Laskowski, R.A., Moss, D.S., Thornton, J.M., 1993. Main-chain bond lengths and bond angles in protein structures. *J. Mol. Biol.* 231, 1049–1067.
- Ma, Q., Sheldrick, G.M., 2005. Thaumatin structure at 1.05 Å resolution. Online available at: <http://molbio.info.nih.gov/cgi-bin/molDraw?1RQW>.
- MacKerell, A.D., Bashford, D., Bellott, M., Dunbrack, R.L., Evanseck, J.D., Field, M.J., Fischer, S., Gao, J., Guo, H., Ha, S., Joseph-McCarthy, D., Kuchnir, L., Kuczera, K., Lau, F.T.K., Mattos, C., Michnick, S., Ngo, T., Nguyen, D.T., Prodhom, B., Reiher, W.E., Roux, B., Schlenker, M., Smith, J.C., Stote, R., Straub, J., Watanabe, M., Wiorkiewicz-Kuczera, J., Yin, D., Karplus, M., 1998. *J. Phys. Chem. B* 102, 3586–3616.
- MOE: molecular operating environment, chemical computing group Inc., Montreal, Canada.
- Min, K., Ha, S.C., Hasegawa, P.M., Bressan, R.A., Yun, D.J., Kim, K.K., 2004. Crystal structure of osmotin, a plant antifungal protein. *Proteins* 54, 170–173.
- Narasimhan, M.L., Coca, M.A., Jin, J., Yamauchi, T., Ito, Y., Kadowaki, T., Kim, K.K., Pardo, J.M., Damsz, B., Hasegawa, P.M., Yun, D.J., Bressan, R.A., 2005. Osmotin is a homolog of mammalian adiponectin and controls apoptosis in yeast through a homolog of mammalian adiponectin receptor. *Mol. Cell* 17, 171–180.
- Neuhaus, J.M., Fritig, B., Linthorst, H.J.M., Meins Jr., F., Mikkelsen, J.D., Ryals, J., 1996. A revised nomenclature for chitinases genes. *Plant Mol. Biol. Rep.* 14, 102–104.
- Neuhaus, J.M., Rogers, J.C., 1998. Sorting of proteins to vacuoles in plant cells. *Plant Mol. Biol.* 38, 127–144.
- Osmond, R.I.W., Hrmova, M., Fontaine, F., Imbert, A., Fincher, G.B., 2001. Binding interactions between barley thaumatin-like proteins and (1,3)-D-glucans. Kinetics, specificity, structural analysis and biological implications. *Eur. J. Biochem.* 268, 4190–4199.
- Reiss, E., Bryngelsson, T., 1996. Pathogenesis-related proteins in barley leaves, induced by infection with *Drechslera teres* (Sacc.) Shoem. and by treatment with other biotic agents. *Physiol. Mol. Plant Pathol.* 49, 331–341.
- Reiss, E., Horstmann, C., 2001. *Drechslera teres*-infected barley (*Hordeum vulgare* L.) leaves accumulate eight isoforms of thaumatin-like proteins. *Physiol. Mol. Plant Pathol.* 58, 183–188.
- Roberts, W.K., Selitrennikoff, C.P., 1990. Zeamatin, an antifungal protein from maize with membrane-permeabilizing activity. *J. Gen. Microbiol.* 136, 1771–1778.
- Selitrennikoff, C.P., 2001. Antifungal proteins. *Appl. Environm. Microbiol.* 67, 2883–2894.
- Schlesier, B., Berna, A., Bernier, F., Mock, H.-P., 2004. Proteome analysis differentiates between two highly homologous germin-like proteins in *Arabidopsis thaliana* ecotypes Col-0 and Ws-2. *Phytochemistry* 65, 1565–1574.
- Sippl, M.J., 1990. Calculation of conformational ensembles from potentials of mean force. An approach to the knowledge-based prediction of local structures in globular proteins. *J. Mol. Biol.* 213, 859–883.
- Trudel, J., Grenier, J., Potvin, C., Asselin, A., 1998. Several thaumatin-like proteins bind to beta-1,3-glucans. *Plant Physiol.* 118, 1431–1438.
- Van Loon, L.C., van Strien, E.A., 1999. The families of pathogenesis-related proteins, their activities, and comparative analysis of PR-1 type proteins. *Physiol. Mol. Plant Pathol.* 55, 85–97.
- Van Loon, L.C., 1985. Pathogenesis-related proteins. *Plant Mol. Biol.* 4, 111–116.
- Vigers, A.J., Robert, W.K., Selitrennikoff, C.P., 1991. A new family of plant antifungal proteins. *Mol. Plant Microbe Interact.* 4, 315–323.
- Wang, H., Ng, T.B., 2002. Isolation of an antifungal thaumatin-like protein from kiwi fruits. *Phytochemistry* 61, 1–6.
- Yun, D.J., Zhao, Y., Pardo, J.M., Narasimhan, M.L., Damsz, B., Lee, H., Abad, L.R., D'Urzo, M.P., Hasegawa, P.M., Bressan, R.A., 1997. Stress proteins on the yeast cell surface determine resistance to osmotin, a plant antifungal protein. *Proc. Natl. Acad. Sci. USA* 94, 7082–7087.
- Yun, D.J., Ibeas, J.I., Lee, H., Coca, M.A., Narasimhan, M.L., Uesono, Y., Hasegawa, P.M., Pardo, J.M., Bressan, R.A., 1998. Osmotin, a plant antifungal protein, subverts signal transduction to enhance fungal cell susceptibility. *Mol. Cell* 1, 807–817.